Influence of nanoparticle morphology and its dispersion ability regarding thermal properties of water used as Phase Change Material

Camila Barreneche[1], Rosa Mondragon[2,*], David Ventura-Espinosa[3], Jose Mata[3], Luisa F. Cabeza[4], A. Inés Fernández[1], J. Enrique Julia[2]

[1]Department of Materials Science and Physical Chemistry, Universitat de Barcelona, Martí i Franqués 1, 08028-Barcelona, Spain

[2]Departamento de Ingenieria Mecanica y Construccion, Universitat Jaume I, 12071-Castellon de la Plana, Spain

[3]Departamento de Química Inorgánica y Orgánica, Universitat Jaume I, 12071-Castellon de la Plana, Spain

[4]GREA Innovació Concurrent, Universitat de Lleida, Edifici CREA, 25001-Lleida, Spain

Corresponding author: mondragn@uji.es

Tel. +34 964 72 81 45 - Fax +34 964 72 81 06

Abstract

Nanoparticles with different morphologies were added to water to study if the morphology of the nanoparticles affects the main parameters of water used as phase change material (PCM). Considered morphologies were spherical, tubes and sheets in the form of spherical carbon black nanoparticles (CB), multiwalled carbon nanotubes (MWCNT), and graphene oxide nanosheets (GO). Results demonstrate that effectively the morphology of nanoparticles affect the thermophysical properties of the nano-enhanced PCM (NePCM). Depending on the morphology of the added nanoparticle, the final NePCM will have different subcooling and thermal conductivity, whereas its phase change enthalpy is not affected and, therefore, is the same for all produced NePCM.

Keywords: Phase Change Material; nanoparticles; morphology; dispersion; water.

1. Introduction

One of the conclusions reached in the 2010 United Nations Climate Change Conference was that Global Warming cannot be avoided, only mitigated [1]. To achieve this objective, efforts should focus on limiting the rise in global temperatures to 2 ºC by 2100. In 2015, the Paris Agreement [2] it was stablished that the 2 ºC reduction target was insufficient, and that a 1.5 ºC target is required. To meet this goal, the emissions levels for 2030 are 55 $GtCO_2e$.

At the current pace of demography and with emerging economies consuming a steadily increasing amount of products and services [3,4], reducing CO_2 emissions relies undoubtedly on innovations in energy technologies to cover energy efficiency, energy harvesting, energy storage, and energy transmission and distribution [5]. These innovations depend on intensifying Research and Development (R&D) activities in forthcoming years to develop an innovative key that enables advanced heat transfer and energy storage materials with market uptake in the mid and long term.

Energy storage technologies can bridge temporal and geographical gaps between energy demand and supply [6]. Energy storage technologies can be implemented on large and small scales in distributed and centralized manners throughout the energy system. While some energy storage technologies are mature, most of them are still in the early stages of development and additional research efforts are needed. The development of affordable thermal energy storage (TES) technologies will improve the efficiency in the use of energy system resources, increase the use of variable renewable resources of energy, raise the self-consumption and self-production of energy, increase energy access (off-grid electrification), improve the electricity grid stability, reliability and resilience, and increase end-use sector of electrification (e.g. electrification of transport sector). Cold TES is an energy saving technology that reduces the electricity peak by storing cold during off peak hours and in seasonal storage [7,8].

TES technologies face some barriers to market entry and in this regard cost is a key issue [9,10]. Cost estimates of TES systems include storage media, system (containers, insulation, heat exchanger, and technical equipment for charging and discharging), and operation costs.

Phase change materials (PCM) can offer high storage capacity associated with the latent heat of the phase change [11,12]. PCM also enable a target-oriented discharging temperature that is set by the constant temperature of the phase change. In addition, in thermal energy storage applications PCM are static, so modular systems ranging from few kW to MW are feasible. However, PCM are not always stable and the boundary conditions of the final application must be controlled [12].

74   One of the most promising approaches to improve PCM properties/behaviour is the addition of well-

75   dispersed nanoparticles [13]. In this case, the PCMs are called nanostructured-enhanced phase change

76   materials (NePCM). Nanoparticles can reduce some of the above mentioned drawbacks, but the two

77   most promising to be reduced are low thermal conductivity and high subcooling, since the particles

78   added have higher thermal conductivity and they can act as nucleation points during the phase change.

79

80   Most NePCM studies have used water, etilenglicol, paraffin wax, and cyclohexane as the base PCM

81   [13,14], most of them for cold storage. Different types of nanoparticles have been used including

82   carbon-based nanostructures (carbon nanofibres, graphite nanoplatelets, singlewalled nanotubes, and

83   multiwalled nanotubes, graphne), oxide-based nanoparticles (Al_2O_3, MgO, TiO_2, and CuO), and

84   metals (Cu, Al, and Ag) [13,15-17]. In some cases, additives were used to improve nanoparticle

85   dispersion and stability [13,18].

86

87   The last studies revealed that when grafted multi-walled nanotube (MWNT) are introduced in

88   paraffin-montmorillonite composite PCM, paraffin molecules are intercalated in the montmorillonite

89   layers and the grafted MWNTs are dispersed by decreasing the latent heat following the mixture rule

90   and increasing 34% the thermal conductivity [19]. Pissello et al. introduced nanoparticles in cement-

91   based composites encouraging results in terms of added functional properties as electrical conductivity

92   and self-sensing potential for a variety of field scopes, e.g. vibration measurements, damage detection,

93   structural health monitoring, electromagnetic shielding, self-heating pavements for deicing and more

94   [20]. In addition, Karaipekli et al. [21] used a perlite matrix where paraffin PCM was impregnated and

95   nanoparticles were added in order to improve the thermal conductivity and results show up to 25%

96   increment and proper durability and reliability.

97

98   As expected, in most cases, the latent heat of NePCM is lowered because of the presence of solid

99   nanoparticles. Although the rule of mixtures can be used to predict the latent heat in most cases [22],

100   some papers report a reduction in the latent heat even below than the one expected by the rules of

101   mixtures [23]. On the other hand, the addition of nanoparticles to PCM can show a strong influence on

102   the fusion temperature. In most of the studies published to date, a noticeable reduction in the fusion

103   temperature is observed. This reduction is due to a PCM-nanoparticle surface interaction [24].

104   However, some authors report no change in phase change temperature [25-26]. In all the studies, a

105   reduction in the degree of subcooling is observed in NePCM.

106

107   But one of the parameters to consider when adding nanoparticles to a PCM is which

108   material/nanoparticle to use and in which morphology, and this has not been clearly studied in the

109   literature so far. The aim of this paper is to investigate if the different morphology of nanoparticles

110   affects the main parameters of the nanofluid when added to a PCM, mainly its dispersion ability.

111   Therefore carbon based nanoparticles with different morphologies (nanoparticles, nanotubes and

112   nanosheets) were added into water to investigate the effect on this PCM. Other parameters that are

113   also influenced by the addition of nanoparticles in water as PCM were also tested, such as the

114   influence in the melting enthalpy, thermal conductivity and subcooling. The shape and size of the

115   nanostructures are important in a way that the surface to volume ratio of nanostructure alters the

116   thermo-physical properties of the PCM [27].

117

118   **2. Materials and methods**

119

120   Water was doped with three different carbon-based nanoparticles:

121   -   Spherical carbon black nanoparticles, CB, were supplied by Cabot Corporation. Commercial

122   nanoparticles ELFTEX 570 consist in amorphous carbon with a primary particle size (dp) of

123   10 nm.

124   -   Multi-walled carbon nanotubes, MWCNT, were purchased from Nanocyl SA. Commercial

125   nanotubes NC7000 present a dp of 9.5 nm and a length of 1.5 μm.

126   -   Graphene oxide nanosheets, GO, were prepared from graphite powder (natural, universal

127   grade, 200 mesh, 99.9995 %) by the Hummers method and were exfoliated using ultrasounds

128   [28]. Final achieved size was 2 nm in diameter and 1 μm in length.

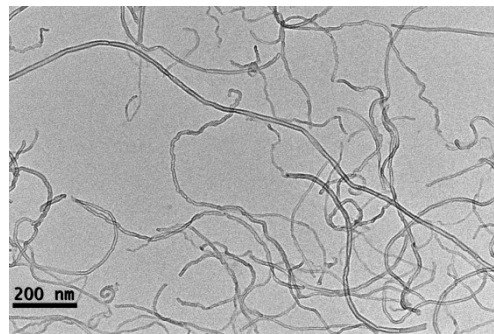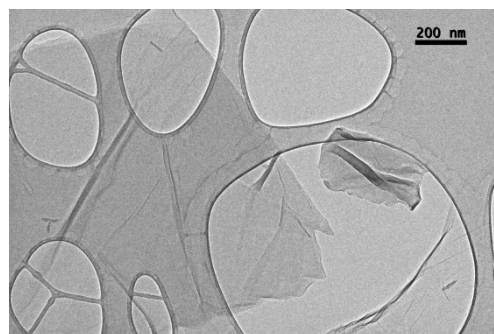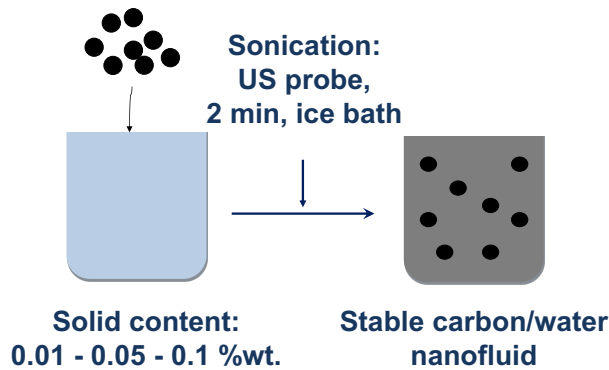129   In Figure 1 TEM images of the primary nanoparticles are shown.

130

(a)

(b)

(c)
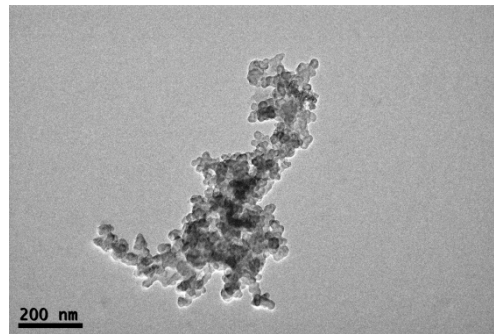
Figure 1. (a) Carbon black, (b) MWCNT, (c) graphene oxide nanosheets

Before the dispersion of the nanoparticles in water, both CB and MWCNT needed to be oxidized with hydrogen peroxide at 120 ºC under magnetic stirring to ensure a good dispersion [29]. Finally, carbon-water NePCM were prepared by introducing the corresponding amount of solid into the water. Three solid mass content (0.01% wt., 0.05% wt., and 0.1% wt.) were tested. The breakage of the agglomerates and the dispersion was achieved by means of a sonication treatment with an ultrasound probe, for 2 minutes at low input energy (15%) in an ice bath to avoid heating of the sample (Figure 2). Ultrasound probes provide the highest degree of dispersion; however the breakage of the agglomerates into primary particles is not ensured. Therefore the final size is the lowest it can be obtained under this conditions but nanoparticles are still agglomerate as it can be observed in the results section. With the aim of comparing the different morphologies, it is important to ensure that all the samples are submitted to the same processing and that they were kept stable although there were

149 clusters of primary nanoparticles. In this case samples were checked to be stable and the clusters
150 present did not settle over time.

151

Solid content: 0.01 - 0.05 - 0.1 %wt.

Sonication: US probe, 2 min, ice bath

Stable carbon/water nanofluid

152
153 **Figure 2. Preparation of the nanocomposite: nanoparticles + PCM**

154

155 The nanoparticles dispersion was characterized by means of the Dynamic Light Scattering (DLS)
156 technique using a ZetaSizer Nano ZS (Malvern Instruments Ltd.). The size distribution of the
157 nanoparticles and agglomerates was obtained for all the samples.

158

159 The phase change enthalpy, temperature and the subcooling reduction were measured by Differential
160 Scanning Calorimetry (DSC) using a DSC2 (Mettler Toledo International Inc.). Approximately 20 mg
161 of sample were introduced in an aluminium crucible sealed in order to avoid loss of material. Samples
162 were submitted to the following cycle: isothermal stage 5 minutes at 20 ºC, cooling from 20 ºC to -25
163 ºC at a cooling rate of 20 ºC·min^{-1}, isothermal stage 5 minutes at -25 ºC, and heating from -25 ºC to 20
164 ºC at a heating rate of 20 ºC·min^{-1}. Three tests were run for each sample and a mean value was
165 obtained.

166

167 Moreover, the thermal conductivity differences between the samples under study were measured by a
168 hot-wire KD2 Pro thermal analyser device using a transient line heat source method [30] to measure
169 effective thermal conductivity. In this method, a thin metallic wire is embedded in the test liquid
170 acting both as heat source and temperature sensor. The transient hot wire technique works by
171 measuring the temperature/time response of the wire to an abrupt electrical pulse. The sample was
172 introduced in a sealed glass tube (20mL) where the sensor was inserted vertically. Measurements were
173 carried out in solid and liquid phase and the tube was immersed in a thermostatic bath with controlled
174 temperature. Eight measurements were performed for each sample, so the experimental error could be
175 determined at 95% of confidence level.

176

177

178

3. Results

Results related with particles size of nanoparticles and nanoparticles clusters are shown in Figure 3. Figure 3 shows the dispersion of the nanoparticles in the different NePCM measured by the DLS. The dispersion of nanoparticles provides information about the available surface area of the nanoparticles inside the PCM. The NePCM based on CB presented agglomeration, so the average size of the CB clusters, assuming spherical shape, is measured. CB nanoparticles dispersion showed almost no dependence with solid mass content and the cluster average values was similar to those found in other experiments [31]. In the case of NePCM based on GO and MWCNT, the results obtained by the DLS were not so conclusive since the primary nanoparticle morphology was not spherical, and the nanoparticle clusters, if present, neither. Consequently, DLS only provided a rough approximation of the nanoparticle dispersion in non-spherical morphologies. It is possible to observe that by using MWCNT better nanoparticle dispersion is achieved than by using GO nanosheets. This fact limits the available nanoparticle surface area in the case of GO-based nanofluids. Differences found in the agglomeration of nanoparticles of different morphologies depend also on the interparticle interactions due to the surface charges that appear in the nanoparticle surface when they are introduced in water. In the GO-based nanofluids attraction forces seem to be higher providing bigger agglomerates in water.
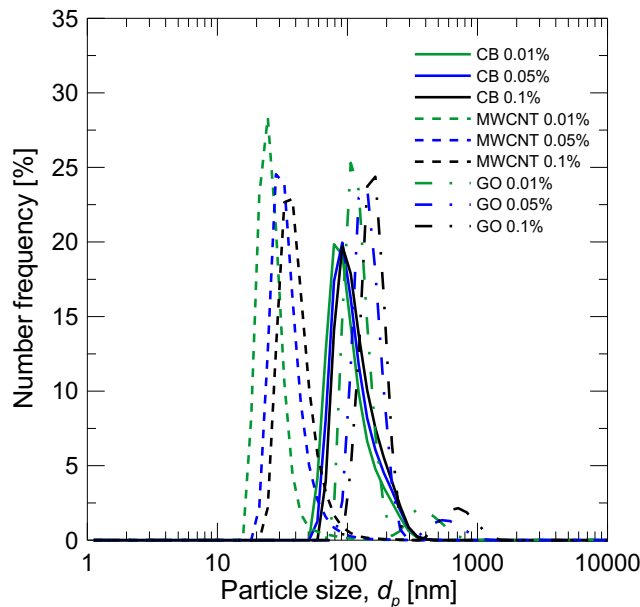

Figure 3. Nanoparticle dispersion degree measured by DLS.

Moreover, it is remarkable that after the same sonication process, the different morphologies studied provide also a different degree of agglomeration. All particle size averages obtained have higher values than those reported for the nanoparticles by themselves with cluster sizes bigger than the nano-scale range, depending on the sample. Differences obtained later in the thermal properties analyzed are mainly due to this cluster formation and the available surface area for each material.

205

206   Otherwise, Figure 4 shows the DSC curves for the NePCM based on CB with different solid mass

207   content. It is possible to observe that there was no noticeable dependence of the melting temperature

208   and phase change enthalpy with the nanoparticle mass content. However, a drastic reduction in the

209   subcooling degree of the NePCM when the nanoparticles content is incremented was observed.

210

211
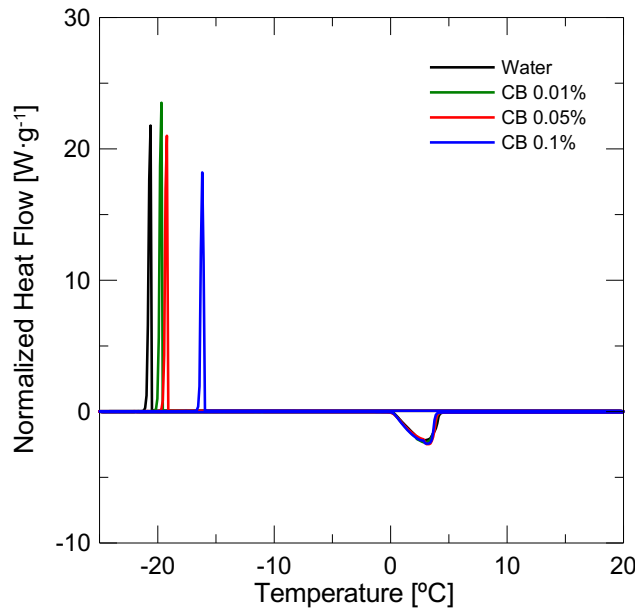
212   **Figure 4.** *DSC curves of NePCM based on CB*

213

214   In order to compare the effect of the different nanoparticle morphologies, Figure 5 shows the phase

215   change enthalpy and subcooling of all the NePCM tested. It is possible to observe that the phase

216   change enthalpy value was almost constant for all the NePCM tested, with values close to the one

217   obtained for the base fluid. However, the subcooling degree depends on the nanoparticle morphology.

218   In the case of CB, it is necessary to use a minimum amount of 0.1% wt. of nanoparticles to get a

219   measurable reduction of subcooling. The maximum reduction of the subcooling for CB is 5 ºC. The

220   maximum reduction of subcooling for MWCNT was only 2.5 ºC, and it was obtained for low solid

221   mass content (0.01% wt.). The reduction of the subcooling with the nanoparticle amount is almost

222   linear for the GO nanosheets with a maximum decrement of 4 ºC.

223
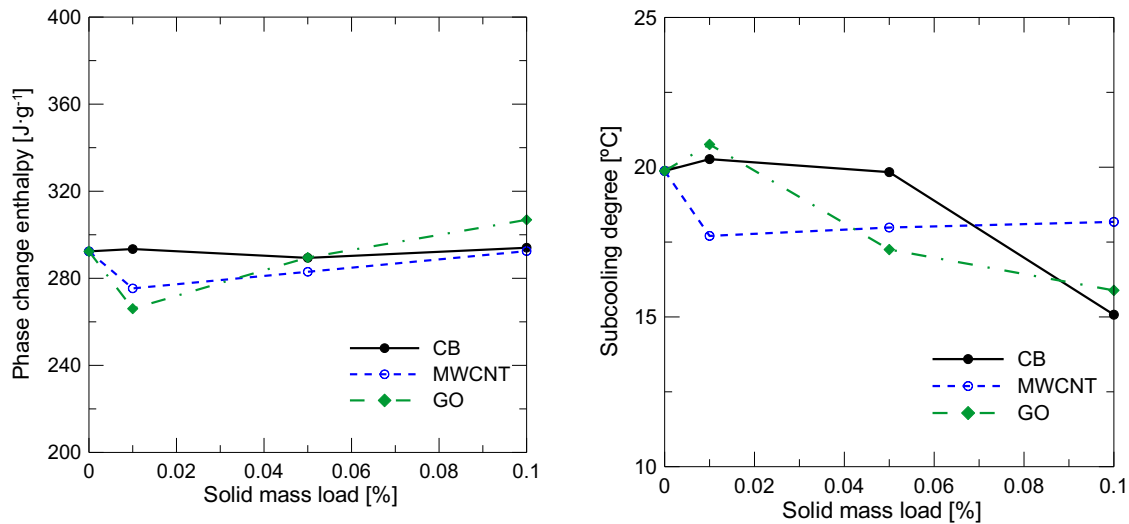
Figure 5. *Left*: *Phase change enthalpy dependence with nanoparticle morphology and solid mass content. Rigth: Subcooling degree dependence with nanoparticle morphology and solid mass content.*

The addition of solid particles with higher thermal conductivity than the base fluid results in a thermal conductivity enhancement that can be predicted by the Maxwell equation [32]. However, according to Gao et al. [33], the enhancement achieved also depends on the size and shape of the particles and clusters of particles in the nanofluid, and deviations from the Maxwell equation results can be found.

The thermal conductivity enhancement measured for the samples under study and its error is shown in Figure 6. Although a general trend of thermal conductivity increment with solid content can be observed, it should be noticed that, as the nanofluids tested have a low particle concentration, the enhancement achieved in liquid phase is negligible for dilute samples. Moreover, for low viscosity fluids the experimental error increases, and the values obtained for thermal conductivity lie within the experimental uncertainty. Only for the highest concentration (0.1% wt.) a maximum enhancement of 2.1% can be found for GO nanofluids. It can be also concluded that in liquid phase, the morphology of the nanoparticles influences the thermal conductivity. For 0.1% wt. solid mass content, nanosheets (GO) present higher conductivity than nanotubes (MWCNT), while the lower value corresponds to spherical nanoparticles (CB). The thermal conductivity enhancement and the morphology dependence measured is in agreement with well stablished equations [32-33].

In solid state, after the phase change, crystallization of water produces a change in the nanoparticle cluster structure. Therefore, the thermal conductivity depends on the cluster size and its morphology, which is expected to be different from the primary particles. Consequently, the formation of clusters of nanoparticles also increases the conduction pathway providing higher enhancements than in liquid

249 phase. In this case, clusters of nanotubes (MWCNT) are the ones with the highest conductivity
250 enhancement, 13.9%.
251
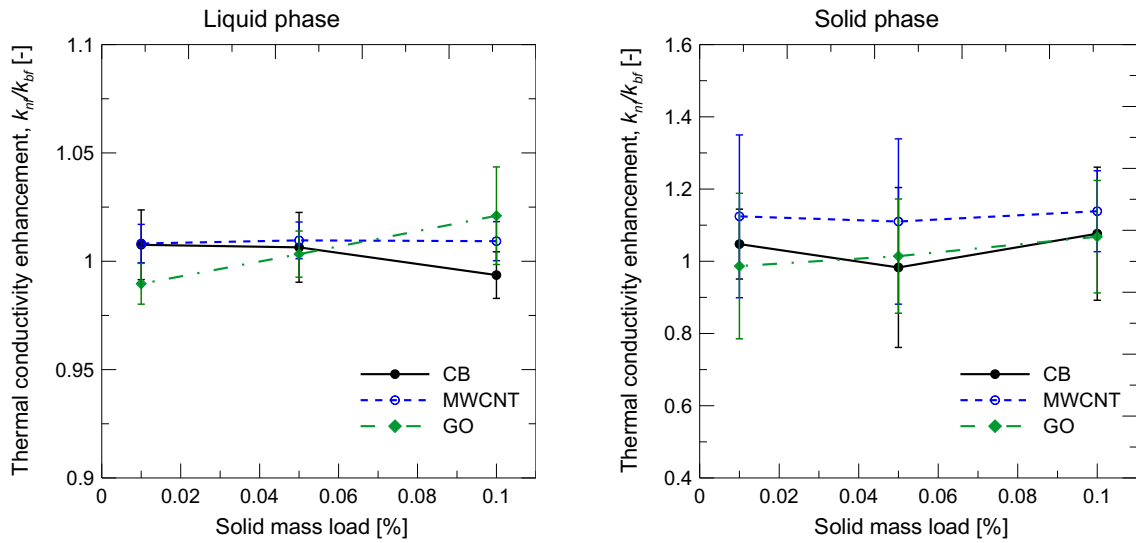
Figure 6. *Thermal conductivity enhancement. Left: Liquid phase. Rigth: Solid phase.*

255 As a general rule the thermal properties depend always on the final size of the agglomerates of
256 nanoparticles. However, for very dilute nanofluids where the interaction among clusters is reduced the
257 influence of the presence of nanoparticles suspended in the base fluid is negligible and independent on
258 the particle geometry. Therefore, only for nanofluids in liquid phase at 0.1% of solid mass load
259 evidences of enhancement of the thermal behaviour can be observed. Otherwise, in solid phase where
260 nanoparticles agglomerate even more during the phase change the influence of the morphology
261 becomes important and nanotubes present the higher increase at any concentration due to the high
262 aspect ratio and the better pathway provided for the transport of phonons responsible for the thermal
263 conductivity enhancement. Moreover, some theoretical models found in the literature to predict this
264 enhancement were modified to include the effect of the higher aspect ratio and are valid only for
265 nanotubes [34].

267 **4. Discussion**

269 Comparing the results obtained in this paper, there are some important highlights detailed as follows:
270 - **CB** presented agglomeration, but **size** showed almost **no dependence with solid mass**
271 **content**. It is possible to obtain a **better nanoparticle dispersion using MWCNT than GO**
272 nanosheets.
273 - There is **no noticeable dependence of the melting temperature** and phase change enthalpy
274 of the PCM with the nanoparticle mass content.
275 - **Subcooling** depends on the nanoparticle morphology:

10

276   • **CB**: it is necessary to use a minimum amount of 0.1% wt. nanoparticles to get a
277   measurable reduction of subcooling. The maximum reduction achieved is **5ºC**.
278   • **MWCNT**: The maximum reduction of subcooling is only **2.5ºC**, and it is obtained for
279   low solid mass content (0.01% wt.).
280   • **GO nanosheets:** The reduction of subcooling with the nanoparticle content is almost
281   linear with a maximum decrement of **4ºC**.
282   -   The **phase change enthalpy** is **almost constant** for all the NePCM tested.
283   -   The **thermal conductivity increment** in solid state is higher when MWCNT nanoparticles are
284   used.
285 Based on the results presented in this paper, Table 1 summarized the results obtained with NePCM
286 containing 0.1% wt. nanoparticles.
287
288   **Table 1. Summary of results obtained for 0.1% wt. NePCMs tested**

Nanoparticles type	Particle size [nm]	Phase change enthalpy [kJ·kg^{-1}]	Subcooling reduction [ºC]	Thermal conductivity increment (solid) [%]
CB	100	291	5	7.6
MWCNT	35	290	2.5	13.9
GO	110	308	4	6.8

289
290
291   **5. Conclusions**
292
293 Different morphologies of nanoparticles were used to study if this fact affects the main parameters of
294 the NePCM when these nanoparticles (CB, MWCNT, and GO) are added to water used as PCM.
295 Results shows that:
296   -   CB/H_2O NePCM agglomerated when it was put in contact with water, the water phase change
297   enthalpy decreased slightly and it had 5 ºC of subcooling reduction (the highest obtained in
298   this study). The thermal conductivity in solid phase increased almost 8% in solid.
299   -   MWCNT/H_2O presented the lowest degree of agglomeration when these nanoparticles were
300   put in contact with water, water phase change enthalpy remained almost equal and it had the
301   lowest subcooling reduction (2.5 ºC). Finally, the thermal conductivity measured showed the
302   highest increment, around 14% in solid phase by the MWCNT addition.
303   -   GO/H_2O presented agglomeration when GO nanoparticles were put in contact with water,
304   phase change enthalpy was almost not affected by the nanoparticles addition and the phase
305   change presented 4 ºC of subcooling reduction. The thermal conductivity increased almost 7
306   % in solid phase.

307 Therefore, the morphology of the nanoparticles affects the NePCM thermophysical properties and this

308 fact must be taken into account when researchers are producing new NePCM.

309

310 To sum up, the nanoparticles type used will change the agglomerate sizes (notice that MWCNT and

311 GO are not spherical and this issue add an uncertainty to the obtained value); the larger the

312 agglomerate, the higher the subcooling reduction taking into account the subcooling decrement. In

313 addition thermal conductivity enhancement also depends on the morphology of the nanoparticles and

314 the clusters formed during the phase change, providing higher values in solid phase. Finally, the phase

315 change enthalpy for dilute nanofluids is fairly affected by the addition of nanoparticles and can be

316 considered to keep constant.

317

318 **Acknowledgements**

319

330

331 **References**

332

333 1. CFR.org "The Global Climate Change Regime". Council on Foreign Relations, 21 July 2012.

334   Web. 16 Feb. 2016.

335 2. Sutter, John D.; Berlinger, Joshua (12 December 2015). "Final draft of climate deal formally

336   accepted in Paris". CNN. Cable News Network, Turner Broadcasting System, Inc. Retrieved 12

337   December 2015.

338 3. Cabeza, L.F., Urge-Vorsatz, D., McNeil, M.A., Barreneche, C., Serrano, S. Investigating

339   greenhouse challenge from growing trends of electricity consumption through home appliances in

340   buildings. 2014. Renewable and Sustainable Energy Reviews 36, 188-193.

341 4. Ürge-Vorsatz, D., Cabeza, L.F., Serrano, S., Barreneche, C., Petrichenko, K. Heating and cooling

342   energy trends and drivers in buildings. 2015. Renewable and Sustainable Energy Reviews 41, 85-

343   98.

344   5. EUROPEAN COMISSION. 2015. A Framework Strategy for a Resilient Energy Union with a
345   Forward-Looking Climate Change Policy.

346   6. S. Kalaiselvam, R. Parameshwaran. Thermal Energy Storage Technologies for Sustainability:
347   Systems Design, Assessment and Applications. Elsevier, USA. ISBN: 978-0-12-417291-3. 2014.

348   7. Oró, E., de Gracia, A., Castell, A., Farid, M.M., Cabeza, L.F. Review on phase change materials
349   (PCMs) for cold thermal energy storage applications. 2012. Applied Energy 99, 513-533.

350   8. Veerakumar, C., Sreekumar, A. Phase change material based cold thermal energy storage:
351   Materials, techniques and applications - A review. 2016. International Journal of Refrigeration 67,
352   271-289.

353   9. IEA-ETSAP, IRENA. Thermal Energy Storage - Technology Brief E17. 2013. Available from:
354   https://www.irena.org/DocumentDownloads/Publications/IRENA-
355   ETSAP%20Tech%20Brief%20E17%20Thermal%20Energy%20Storage.pdf (16/02/2016)

356   10. SHC-Task 42, ECES-Annex 29. Compact Thermal Energy Storage IEA SHC Position Paper.
357   2015. Available from: https://www.iea-shc.org/data/sites/1/publications/IEA-SHC-Compact-
358   Thermal-Storage-Position-Paper.pdf (16/02/2016).

359   11. Farid, M.M., Khudhair, A.M., Razack, S.A.K., Al-Hallaj, S. A review on phase change energy
360   storage: Materials and applications. 2004. Energy Conversion and Management 45 (9-10), 1597-
361   1615.

362   12. Cabeza, L.F., Castell, A., Barreneche, C., De Gracia, A., Fernández, A.I. Materials used as PCM
363   in thermal energy storage in buildings: A review. 2011 Renewable and Sustainable Energy
364   Reviews 15 (3), 1675-1695.

365   13. Kaviarasu, C., Prakash, D. Review on phase change materials with nanoparticle in engineering
366   applications. 2016. Journal of Engineering Science and Technology Review 9 (4), 26-386.

367   14. Mondragón R., Martínez-Cuenca R., Hernández L., Andreu-Cabedo P., Cabedo L., Julià J.E.
368   Handbook of Clean Energy Systems, Volume 5 - Energy Storage: Thermal Energy Storage;
369   Chemical Storage; Mechanical Storage; Electrochemical Storage; Integrated Storage Systems.
370   Chapter 33 – Nanotechnology and Nanomaterials for thermal energy storage. Editor-in-chief:
371   Jinyue Yan. Wiley, UK, 2015. ISBN: 978-1-118-38858-7.

372   15. Li, Y., Zhou, J., Tung, S., Schneider, E., Xi, S. A review on development of nanofluid preparation
373   and characterization. 2009. Powder Technology 196 (2), 89-101.

374   16. Sidik, N.A.C., Mohammed, H.A., Alawi, O.A., Samion, S. A review on hybrid nanofluids: Recent
375   research, development and applications. 2014. International Communications in Heat and Mass
376   Transfer 54, 115-125.

377   17. Sathishkumar, A., Kumaresan, V., Velraj, R. Solidification characteristics of water based graphene
378   nanofluid PCM in a spherical capsule for cool thermal energy storage applications. 2016.
379   International Journal of Refrigeration 66, 73-83.

13

380   18. Wang, J., Xie, H., and Xin, Z. Thermal properties of heat storage composites containing
381   multiwalled carbon nanotubes. 2008. Journal of Applied Physics 104, 113537–113545.

382   19. Li, M., Guo, Q., Nutt, S. 2017. Carbon nanotube/paraffin/montmorillonite composite phase
383   change material for thermal energy storage. Solar Energy 146, 1–7.

384   20. Pisello, A.L., D'Alessandro, A., Sambuco, S., Rallinic, M., Ubertinia, F., Asdrubalia, F.,
385   Materazzic, A.L., Cotana F. 2017. Multipurpose experimental characterization of smart
386   nanocomposite cement-based materials for thermal-energy efficiency and strain-sensing
387   capability. Solar Energy Materials & Solar Cells 161, 77–88.

388   21. Karaipekli, A., Biçer, A., Sarı, A., Tyagi, V. 2017. Thermal characteristics of expanded
389   perlite/paraffin composite phase change material with enhanced thermal conductivity using carbon
390   nanotubes. Energy Conversion and Management 134, 373–381.

391   22. Zeng, J.L., Cao, Z., Yang, D.W., et al. Thermal conductivity enhancement of Ag nanowires on an
392   organic phase change material. 2010. Journal of Thermal Analysis and Calorimetry 101, 385–389.

393   23. Wu, S., Zhu, D., Zhang, X., and Huang, J. Preparation and melting/freezing characteristics of
394   Cu/paraffin nanofluid as phasechange material (PCM). 2010. Energy and Fuels 24, 1894–1898.

395   24. Hong, H., Wensel, J., Peterson, S., and Roy, W. Efficiently lowering the freezing point in heat
396   transfer coolants using carbon nanotubes. 2007. Journal of Thermophysics and Heat Transfer 21,
397   446–448.

398   25. Ho, C.J. and Gao, J.Y. Preparation and thermophysical properties of nanoparticle in paraffin
399   emulsion as phase change material. 2009. International Communications in Heat and Mass
400   Transfer 36, 467–470.

401   26. Kumaresan, V., Velraj, R., and Das, S.K. The effect of carbon nanotubes in enhancing the thermal
402   transport properties of PCM during solidification. 2012. Heat and Mass Transfer 48, 1345–1355.

403   27. Parameshwaran R., Kalaiselvam S.. Nanomaterial-embedded phase-change materials (PCMs) for
404   reducing building cooling needs. 2015. Eco-efficient Materials for Mitigating Building Cooling
405   Needs 401–443.

406   28. Hummers, W. S.; Offeman, R. E. 1958. Preparation of Graphitic Oxide. Journal of the American
407   Chemical Society 80, 1339-1339.

408   29. Han, D.X., Meng, Z.G., Wu, D.X., Zhang, C.Y., Zhu, H.T. Thermal properties of carbon black
409   aqueous nanofluids for solar absorption. 2011. Nanoscale Research Letters 6, 457, 1-7.

410   30. Mujumdar, A. S. Handbook of Industrial Drying. Third Edition 25 (6). CRC Press 2006.

411   31. Mondragon, R., Segarra, C., Martınez-Cuenca, R., Julià E, Jarque JC. Experimental
412   characterization and modeling of thermophysical properties of nanofluids at high temperature
413   conditions for heat transfer applications. 2013. Powder Technology 249, 516–529.

414   32. Maxwell J C. A Treatise on Electricity and Magnetism 1873, Clarendon Press Oxford

415   33. Gao J W, Zheng R T, Ohtani H, Zhu D S and Chen G. Experimental investigation of heat
416   conduction mechanisms in nanofluids. Clue on clustering. 2009. Nano Letters 9 (12) 4128-32.

14

417   34. Yang, L., Xu, J., Du, K., Zhang, X. 2017. Recent developments on viscosity and thermal
418   conductivity of nanofluids. Powder Technology 317, 348–369.